ELSEVIER

Ceramics International 31 (2005) 599–610

CERAMICS INTERNATIONAL

www.elsevier.com/locate/ceramint

Synthesis and sintering behaviour of spinel-type $Co_xNiMn_{2-x}O_4$ ($0.2 \leq x \leq 1.2$) prepared by the ethylene glycol–metal nitrate polymerized complex process

P. Durán[a,*], J. Tartaj[a], F. Rubio[a], C. Moure[a], O. Peña[b]

[a] *Instituto de Cerámica y Vidrio (CSIC)—Campus de Cantoblanco, Camino de Valdelatas s/n, 28049 Madrid, Spain*
[b] *Chimie du Solide et Inorganique Moleculaire, UMR 6511, CNRS—Université de Rennes I, Institut de Chimie de Rennes, 35042 Rennes Cedex, France*

Received 16 April 2004; received in revised form 1 July 2004; accepted 22 July 2004
Available online 8 December 2004

Abstract

$Co_xNiMn_{2-x}O_4$ ($0.2 \leq x \leq 1.2$) spinel-type powders were prepared by auto-combustion of ethylene glycol–metal nitrate polymerized gel precursors. A pure spinel-type phase, with no intermediate compounds, was attained from the burning of the polymerized gel precursor and subsequent calcining at 600–700 °C. The formation and the structural evolutions of the spinel-type phase have been studied by simultaneous thermogravimetric and differential thermal analysis (TG/DTA), X-ray diffraction (XRD), Fourier transform infrared (FTIR) spectroscopy, Brunauer–Emmett–Teller (BET), scanning electron microscopy (SEM), and transmission electron microscopy (TEM). Powder characteristics such as particle size and specific surface areas of the calcined powders were dependent of the chemical compositions. In the same way, the crystalline structure of the synthesized spinel-type phases was strongly dependent of the Co content, and a tentative cationic distribution is proposed. Sintering of the $Co_xNiMn_{2-x}O_4$ oxides have been studied by both the constant rate of heating (CRH) and the conventional ramp-and-holding methods. Density increased with the increasing of the Co content, and theoretically dense bodies (≥99.9% of the theoretical density) with submicronic average grain sizes were obtained at a temperature as low as 1050 °C for 6 h in the case of the $Co_{1.2}NiMn_{0.8}O_4$ composition. Above that temperature, and coinciding with the apparition of an amorphous cobalt oxide liquid-phase, a slow bloating phenomena as consequence of the evolution of oxygen gas with the corresponding decreasing in density and the beginning of an exaggerated grain growth in the sintered samples was present. Microstructural evolution of the samples as a function of the sintering temperature has also been studied.

Keywords: A. Powders: chemical preparation; A. Sintering; D. Spinels

1. Introduction

Complex spinel oxides based on transition metals such as Co, Ni, and Mn are of significant interest from both a fundamental point of view because of their structural and unusual magnetic properties and, on the other hand, owing to their technological applications as negative temperature coefficient (NTC) thermistors for temperature measurement and control. The magnetic properties are widely determined by the distribution of cations located between the tetrahedral (A) and the octahedral (B) sites of the spinel structure (AB_2O_4).

In view of the changes of crystal structure on cooling high temperature sintered samples, the cation distribution has been found to be affected by several factors and, between them, the preparation and thermal history are two of the most important. In order to obtain single-phase cubic spinel oxide, Abe et al. [1] proposed a new method for the Co–Ni–Mn–O ternary system. Firstly the region of single-phase cubic spinel-type in the ternary system was studied, and then the oxide compound was oxidized at the temperatures where the

* Corresponding author. Tel.: +34 91 735 58 54; fax: +34 91 735 58 43.
E-mail address: pduran@icv.csic.es (P. Durán).

0272-8842/$30.00
doi:10.1016/j.ceramint.2004.07.007

spinel structure is stable [2,3]. The study was restricted to the compositions in which the Mn/Co/Ni molar ratios were 2/4/0 and 4.5/0/1.5. Given that the cubic spinel phase is unstable at high temperature, a better processing method would be desirable to sinter the NTC materials at moderate temperatures with a high densification level avoiding, thus, the segregation phases phenomenon present on cooling in high temperature sintered samples. In such a way de Vidales et al. [4] carried out an alternative preparation route using the coprecipitation of the Co, Ni, and Mn cations with *n*-butylamine. The as prepared powders were highly sinterable, and dense bodies (96% of the theoretical density) at a temperature as low as 1000 °C were attained. Other preparation methods using the evaporation to dryness of the nitrates or coprecipitation have also been proposed [5,6].

In the present paper we tried to synthesize at low-temperature cubic spinel single-phase in the Co–Ni–Mn oxides ternary system using a (presumably) cation chelating organic compound as the ethylene glycol. The study of the complex polymeric (chelates) decomposition, thermal evolution, powders morphology and structural characterization by FTIR, DTA/TG, X-ray diffraction, BET specific surface areas, and SEM and TEM observations on the as prepared powders have been carried out. The sintering behaviour by the constant rate of heating (CRH) method of $Co_xNiMn_{2-x}O_4$ samples and microstructure are reported.

2. Experimental procedure

A series of mixed oxides $Co_xNiMn_{2-x}O_4$, where $0.2 \leq x \leq 1.2$, were prepared. In the present work, the compositions $Co_{0.2}Ni_{1.0}Mn_{1.8}O_4$, $Co_{0.6}Ni_{1.0}Mn_{1.4}O_4$, and $Co_{1.2}Ni_{1.0}Mn_{0.8}O_4$ referred to as 218, 614, and 1218, respectively, were prepared. The powders of $Co(NO_3)_2{\cdot}6H_2O$ $6H_2O$ (15.768 g), $Ni(NO_3)_2{\cdot}6H_2O$ (13.135 g), and $Mn(NO_3)_2{\cdot}4H_2O$ (9.068 g), in the case of the 218 compositions, were dissolved in 20 ml of distilled water. To the aqueous solutions of metal nitrates was added concentrated nitric acid (65%) (10 ml) by stirring at room temperature. Then ethylene glycol (EG) (80 ml) to make a gel was added by stirring. This gel and those heat-treated at 60–80 °C for 16 h, and that dried at 130 °C for 24 h will be referred to as 218-0, 218-80, and 218-130, respectively. For comparison, a blank solution of pure ethylene glycol, EG, was used. After drying the gel was fired at 750 °C in air for 2 h. The same preparation pathway was used for the 614 and 1218 spinel compositions, using the required chemical equivalents in each case.

The decomposition and reaction processes of the dried polymeric gel were analyzed by simultaneous thermogravimetric and differential thermal analysis TG/DTA (Model STA 409, Netzsch, Germany) in the temperature range from room temperature to 1000 °C in air with a heating rate of 10 °C/min. To study the phase transformation, crystallization and sinterability of the derived powders, the complex polymeric gel were decomposed at various temperatures for 2 h. The complex polymeric gel and derived powders were also analyzed by Fourier transform infrared (FTIR) spectroscopy (Model 1760 X, Perkin-Elmer, Norwalk, CT, USA). The crystallization and microstructure of the oxide powders were characterized with an X-ray diffractometer (XRD) (Model D-5000, Siemens, Erlangen, Germany) using CuK radiation. A scanning electron microscope (SEM) (Model DSM 950, Karl Zeiss, Oberkochem, Germany), and a transmission electron microscope (TEM) (Model H-7000, Hitachi, Tokyo, Japan) were used to study the morphology and agglomeration state of the calcined powders. Specific surface areas of the oxide powders was measured by the single-point Brunauer–Emmet–Teller (BET) method using N_2 gas (Model MS-16, Quantachrome Corp, Suoset, NY, USA), and was converted to particle/crystallite size according to the following equation assuming that the particles are closed spheres with smooth surface and uniform size:

$$D_{\mathrm{BET}} = \frac{6 \times 10^3}{d_{\mathrm{th}} S_{\mathrm{BET}}}$$

where d_{th} is the theoretical density of the powder (g/cm^3), D_{BET} (nm) the average particle/crystallite size, and S_{BET} the specific surface area expressed in m^2/g. Before compaction, the particle size distribution of the $Co_xNiMn_{2-x}O_4$ precursor powders, previously calcined at 750 °C for 2 h and attrition milled for 2 h, was studied by the sedimentation technique.

The sintering behaviour of the spinel-type samples was studied, on the calcined powders isopressed at 200 MPa, with a dilatometer (Model 402E/7, Netzsch, Germany) in a still-air atmosphere at a constant rate of heating (CRH) of 5 °C/min. On the other hand, isopressed pellets were also sintered in air under isothermal conditions at 900–1200 °C for 6 h. The heating and cooling rates were 2 °C/min. The density of the sintered samples was measured by the Archimedes method in water.

Microstructure of the sintered samples was observed with a scanning electron microscope (SEM) and a transmission electron microscope (TEM) on the gold coated fracture surfaces, and the average grain size was determined by the linear intercept method.

3. Experimental results

3.1. Study of the precursor thermal behaviour

Fig. 1 shows the TG/DTA curves for the different prepared compositions. During the heating of the dried polymeric gel between room temperature and 1000 °C, several thermal features take place leading to a better knowledge of the spinel formation reaction mechanism. The TG curve of Fig. 1(a) shows for all the compositions three well-defined weight loss steps. In the first one a continuous loss of about 33 wt%, between room temperature and about 250 °C, took place. Such a weight loss can be related with the drying process of the polymeric gel. In the second weight

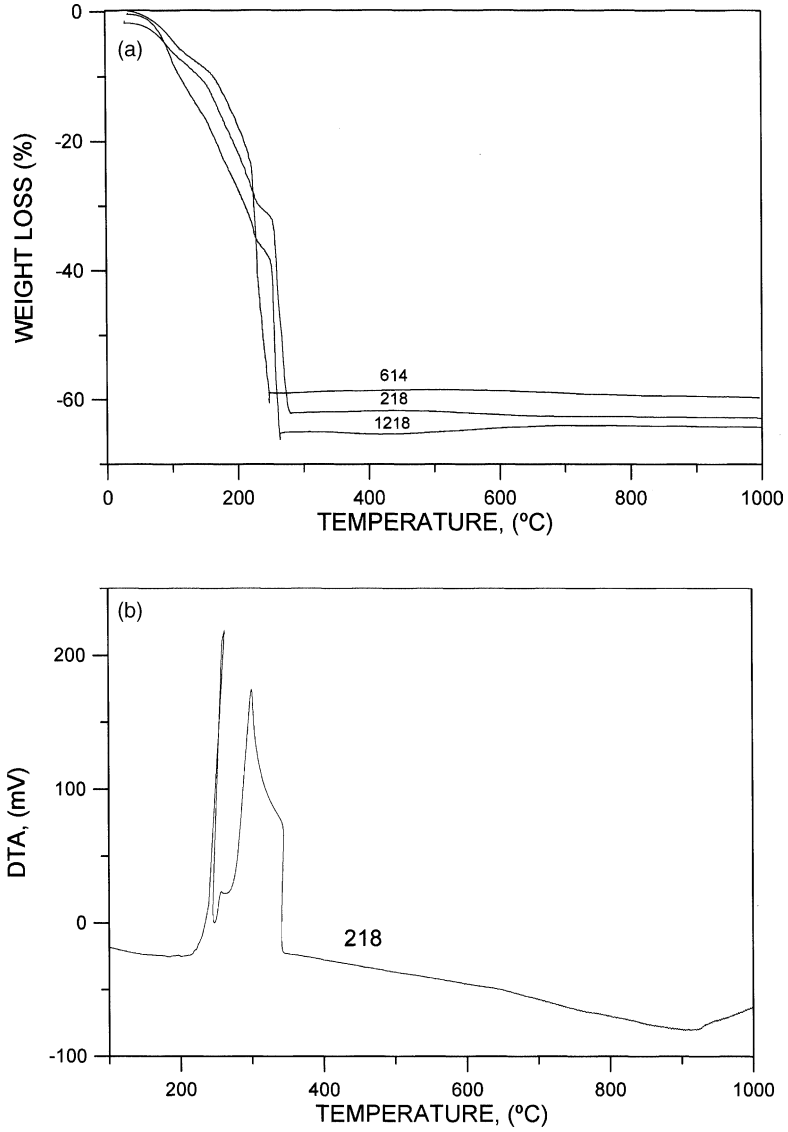

Fig. 1. (a) TG and (b) DTA curves for the 218, 614, and 1218 spinel polymeric gel precursors.

loss step, above 250 °C, a drastic weight loss of about 30% more occurred. This second weight loss takes place in a very narrow temperature range, and indicates that an auto-combustion occurs during the heating of the metal nitrate–ethylene glycol polymerized complex dried gel. In the third step, a continuous and variable in amount of weight gain between the end of the auto-combustion process and about 600 °C, was also present in all compositions. Such a weight gain can be related to the formation of Co_3O_4 from CoO. Above that temperature the weight loss remained almost constant. The overall combustion reaction in air could be represented as follows:

$$m[(Co_{0.2}NiMn_{1.8})(NO_3)_2 \cdot H_2O]_s + n[HOCH_2 - CH_2OH]_1 \rightarrow [mN_2 + 2nCO_2 + (m + 2n)H_2O]_g \uparrow + m[(Co_{0.2}NiMn_{1.8})O_4]_s$$

In the temperature range in which the main weight changes took place, i.e., between room temperature and about 600 °C, the DTA curve showed five thermal effects in all the compositions. For simplicity, only that corresponding to the 218 composition is shown in Fig. 1(b). A smooth and broad endothermal effect, between room temperature and about 230 °C, followed by a narrow exothermic peak with its maximum at 260 °C, associated with a shoulder at about 262.5 °C, were present. A new and strong exothermic peak at 300 °C and its associated shoulder at about 340 °C were also present in the DTA curve. It may be noted that apparently no weight loss accompanies the two last exothermal effects. Finally, above 920 °C an exothermic effect began to appear which is related to the reduction of Co_3O_4 to CoO with liberation of oxygen.

From the whole of the above thermal features, the reaction mechanism leading to the formation of the spinel-

type $Co_xNiMn_{2-x}O_4$ phase would be carried out in three well-established steps: (i) in the first one the drying of the polymerized gel with the probable formation of an EG-metal nitrate polymerized complex is produced, (ii) in the second one an auto-combustion of the metal nitrate–ethylene glycol followed by the oxidation of the evolved gases takes place and, finally, (iii) in the third step, a reaction and crystallization of the decomposed metal nitrate–ethylene glycol polymeric dried gel to form the spinel-type phase takes place. The no weight loss accompanying the strong exothermic effect occurring at this third stage supported the above contention.

3.2. The formation of the $Co_xNiMn_{2-x}O_4$ spinel-type crystal structure

In order to support such a belief, different samples of the polymeric dried gel were heated to different temperatures, which coincided with the completion of the most important TG steps and DTA features. X-ray diffraction (XRD), FTIR spectroscopy, SEM, and TEM microscopy observations characterized the as obtained powders.

Fig. 2 shows the XRD patterns of the 218 composition samples fired at 263, 300, 342, 400, 500, 640 and 750 °C for 2 h. When the polymeric gel was heated at 263 °C an almost amorphous XRD pattern was recorded, but some peaks (rather broad bands) centered at 35.7, 43.4, and 63.2 in 2θ could be attributed to an incipient formation of the spinel phase. At 400 °C, all the peaks of the XRD pattern were completely indexed as the spinel-type manganite, but those fired below 260 °C could not be indexed as the spinel-type manganite. Therefore, it is considered that the exothermic peak at about 300 °C in the DTA curve, Fig. 1(b), was caused by the crystallization from pure amorphous oxide possessing the spinel-type manganite composition. As the temperature treatment increased the larger the peak intensity and narrower the peaks suggesting, thus, that the spinel-type crystalline phase became more perfect. In agreement with literature data, the crystallographic data for the well-crystallized spinel phases synthesized at 850 °C for 4 h were evaluated as the following: $a = 0.8372$ nm, and $a = 0.8323 \pm 0.0001$ nm, according to a cubic symmetry, $Fd3m$ space group and $Z = 8$, for the 218 and 614 spinel compositions, and $a = 0.5835$ nm and $c = 0.8423 \pm 0.0001$ nm according to a tetragonal symmetry, $I41/amd$ space group and $Z = 4$, for the 1218 composition. When compared with a conventional solid-state reaction, using the metal nitrate–ethylene glycol process strongly lowered the spinel-phase synthesis temperature.

Fig. 3 shows the FTIR spectra of the as prepared EG–metal nitrate–water–nitric acid solution 218-0 and of its

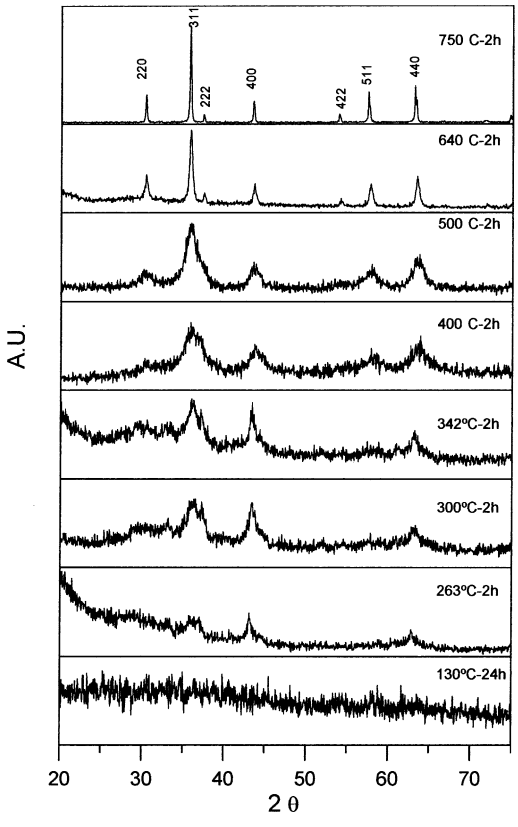

Fig. 2. XRD patterns showing the phase evolution in the 218 spinel polymeric gel dried at 130 °C, and then calcined at the indicated temperatures.

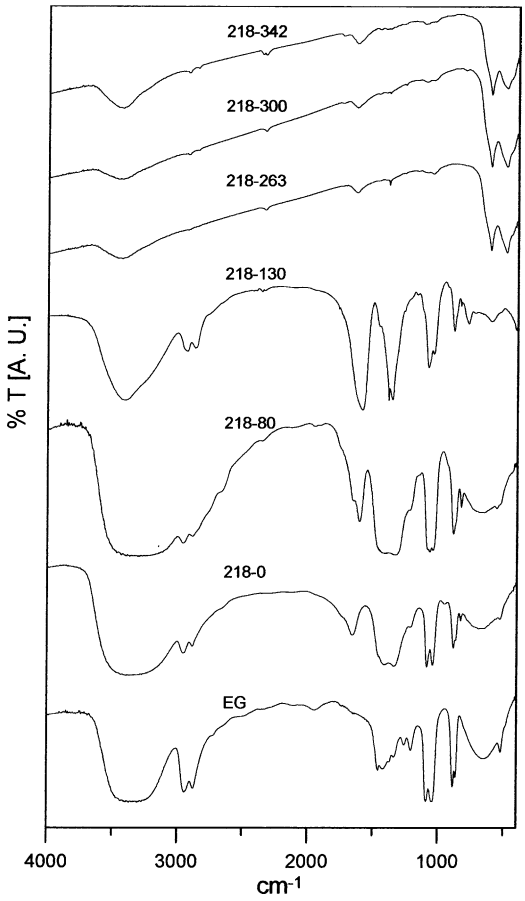

Fig. 3. FT-IR transmission spectra of the 218 spinel polymeric gel before heating and heated at the indicated temperatures.

decomposition products at selected temperatures. The IR spectrum of the 218-0 solution, i.e., without heat-treatment, was quite complex but a broad absorption band at about 3400 cm^{-1} attributable to the stretching vibration of the hydrogen-bonded O–H groups, was present. The absorption band at 2930–2870 cm^{-1} is attributed to the stretching vibration mode of the CH_2 group of which low intensity can be attributed to a probable partial oxidation of ethylene glycol. An absorption band at about 1650 cm^{-1} can be due to the stretching vibration of the free O–H group of water. The carboxylate anion (COO^-) stretching is also shown by the appearance of a small absorption band at 1730 cm^{-1} and the strong absorption band at 1338 cm^{-1} [7]. The bands located at 1455, 1080–1030 and 885 cm^{-1} indicate the presence of nitrate ions in the polymeric gel. After the heat-treatment at 80 °C no appreciable changes were observed in the IR spectrum, but new absorption bands at about 1600, 1417, 1065 and 650–554 cm^{-1} were present. These new absorption bands seem to correspond to the C=O groups, carboxylate anions, and metal–oxygen bonds, respectively, in the complex gel structure. An intensity decreasing or increasing in the absorption bands correspponding to the CH_2 groups and the O–C=O group, respectively, was also observed. After 24 h standing time at 130 °C, the presence of an absorption band at 775 cm^{-1} could be attributable to the existence of some formate and/or oxalate ions, although such an assumption was not confirmed by the XRD results. Finally, the absorption band at about 600 cm^{-1} can be attributed to the presence of metal–oxygen bonds in the complex gel structure. When the polymeric gel was heated at 263 °C, the intensity of the bands at 2930–2870 cm^{-1} diminished or disappeared, indicating the total oxidation of the ethylene glycol. The absorption bands corresponding to the carboxylate and carboxylic acid groups (–COO) and (–COOH) still remained. After heating at 340 °C, i.e., at the completion of the total weight loss, all the previously mentioned absorption bands have practically disappeared, and only strong absorption bands at about 500 and 600 cm^{-1} due to the metal–oxygen bonds were observed.

3.3. Morphology and characterization of the spinel-type powders

Fig. 4(a)–(c) shows representative SEM photomicrographs of the 218 polymeric gel calcined at different temperatures. In a general sense, all the powder compositions calcined at 263 °C showed the morphology of hardened round hollow spherical agglomerates containing pores and voids caused by the scaping gases during the violent combustion process, as shown in Fig. 4(a). Fig. 4(b) and (c) show the microstructure of the spherical agglomerates surfaces, after heating at 400 °C, in which the primary spinel phase particle can be observed. The individual particles were a few tens of nanometer in size with a high agglomeration state, larger in the case of the 614 spinel composition. The powder morphology of the polymeric gel

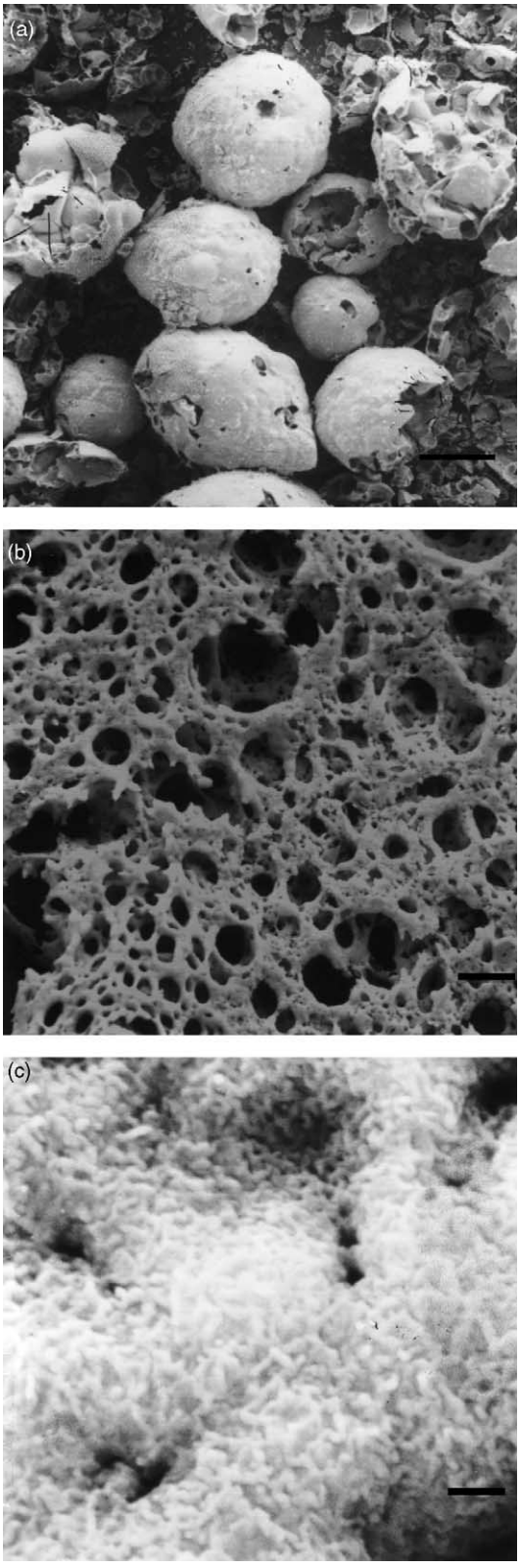

Fig. 4. SEM micrographs of the 218 polymeric gel precursors calcined at 263 °C, (a) (bar = 200 μm) and microstructure of the polymerized gel precursors calcined at 400 °C, (b) (bar = 10 μm) and (c) (bar = 0.5 μm).

calcined at 400 °C, i.e., after the completion of the weight loss, were made of agglomerates of about the same size and shape of those calcined at lower temperatures. Each one of these agglomerates, which were much larger than the crystal size, consisted of nanometric particle in the case of the 218 spinel composition. In the case of the 614 spinel composition the particles were submicronic in size, i.e., some particle growth took place at that calcining temperature. The BET specific surface areas of the powders calcined at 400 °C ranged from about 35 $m^2 g^{-1}$ in the case of the 218 composition up to 12 $m^2 g^{-1}$ for the 1218 composition. After calcining at 750 °C, the BET specific surface areas decreased up to 5 and 9.5 $m^2 g^{-1}$, respectively. These results indicated a high sinterability of the spinel-type calcined powders.

The influence of the calcination temperature on the grain size of the spinel-type powders has also been studied by transmission electron microscopy (TEM). This study revealed that the agglomeration state was much lower in the case of the 218 sample than in the other two spinel-type compositions. The average grain size in the case of the 218 composition calcined at 400 °C was determined to be about 15 nm. In a general sense, the morphology of the agglomerates was of small primary spinel-type particles with a high level of interconnected internal porosity. The crystallinity of the powder was more perfect with increasing temperature, and the particle size also increased up to 18 and 35 nm at 500 and 640 °C, respectively. The grain size grew quickly up to about 100 nm when the temperature raised to 750 °C. For simplicity again, Fig. 5(a)–(c) show the grain

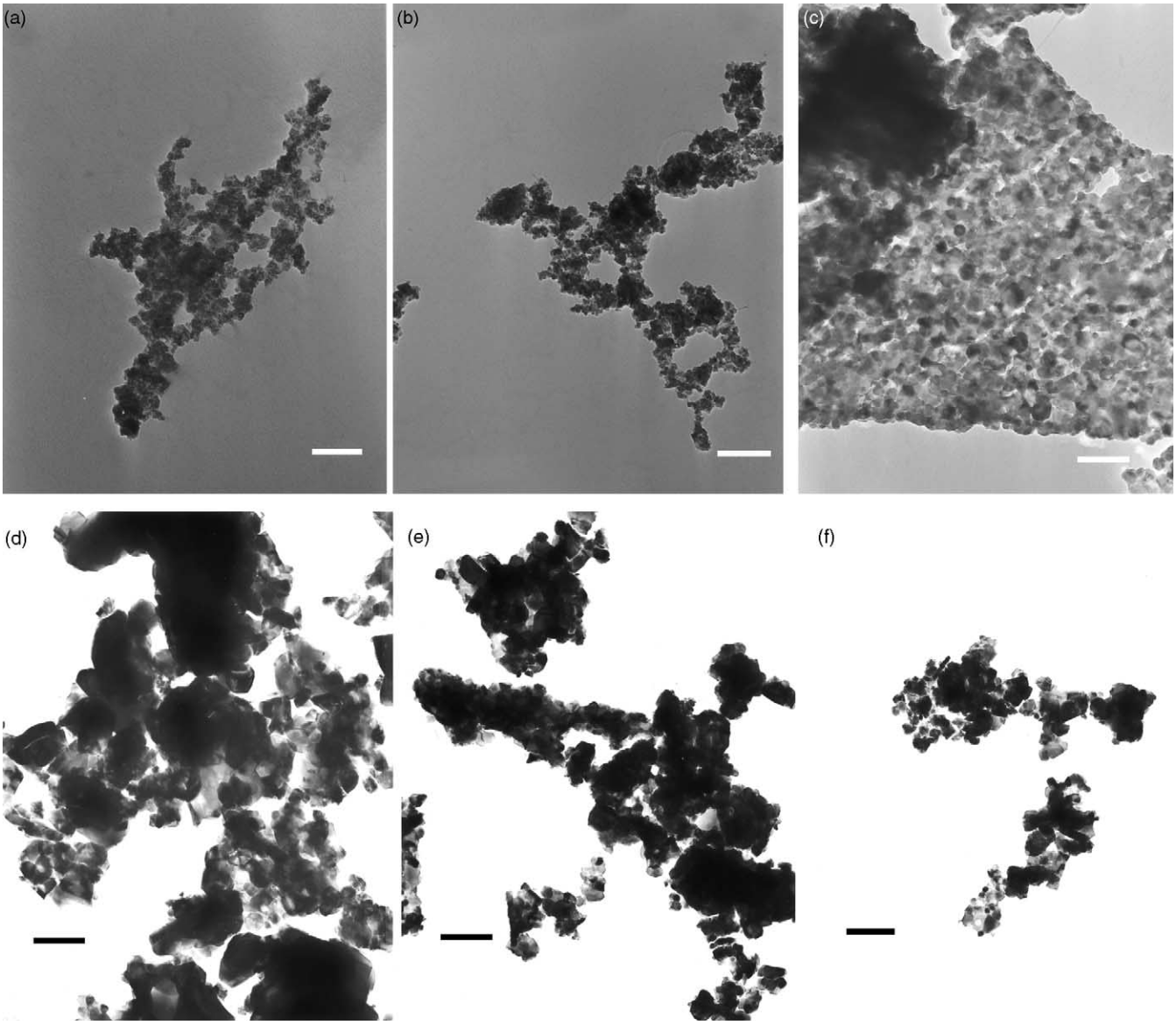

Fig. 5. TEM micrographs of the 614 spinel polymeric gel precursors calcined at 400, 500, and 640 °C (a) to (c) (bar = 0.2 μm), and those of the 218, 614, and 1218 spinel powder compositions calcined at 750 °C (d) to (f) showing the different agglomeration state of the powders (bar = 0.5 μm).

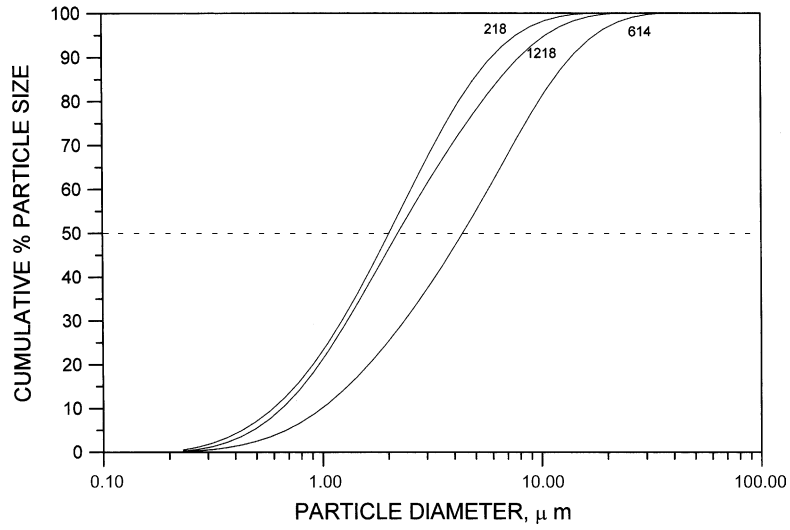

Fig. 6. Particle-size distributions of calcined 218, 614 and 1218 spinel powders after attrition milling.

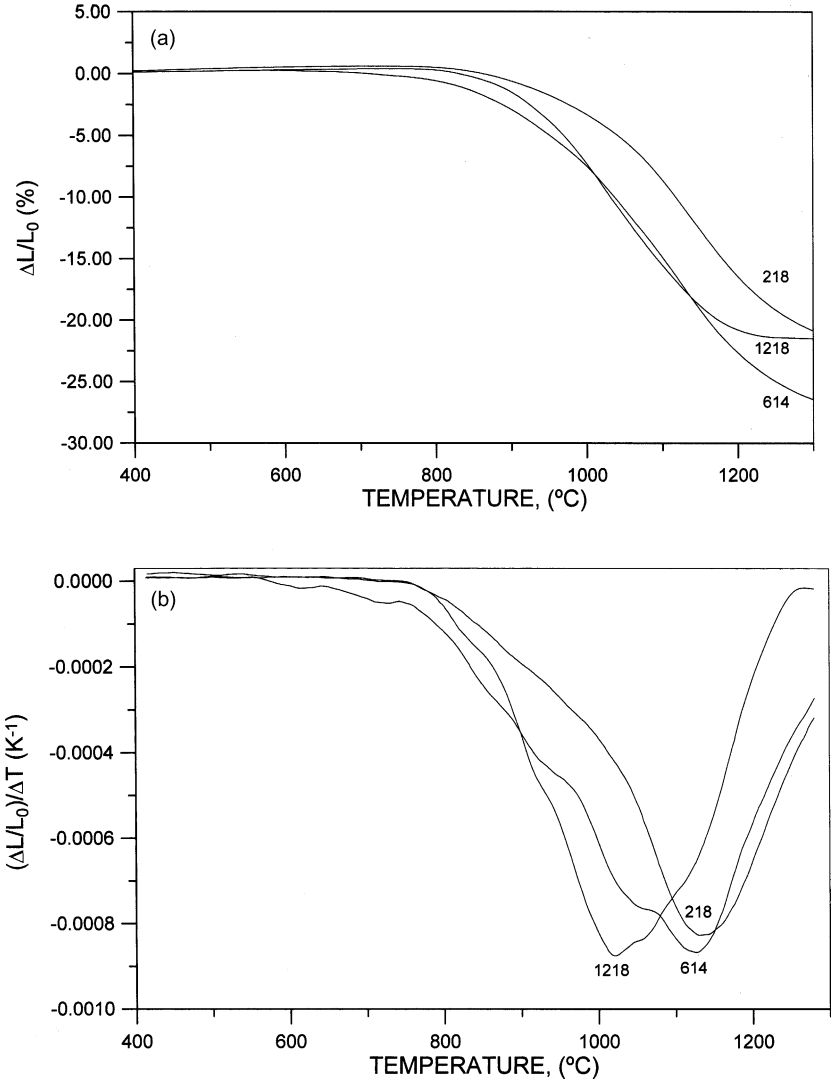

Fig. 7. CHR sintering behaviour of $Co_xNiMn_{2-x}O_4$ spinel powder compacts: (a) linear shrinkage and (b) linear shrinkage rate as a function of temperature.

size evolution with calcination temperature between 400 and 640 °C only for the case of the 614 spinel powder composition, and Fig. 5(d)–(f) show the grain size of the three spinel powder compositions after calcining at 750 °C for 2 h. By comparison the grain sizes measured by TEM with those calculated from SEM observations and the BET specific surface areas, we conclude that the particle size measured by the two last methods corresponded, as above stated, to that of the agglomerates, i.e., the grain sizes were larger that the crystal sizes because the powder particles were made of several crystallites.

3.4. Sintering behaviour of the $Co_xNiMn_{2-x}O_4$ oxides

A sintering study of the $Co_xNiMn_{2-x}O_4$ fine particle was carried out by compacting the powders isostatically at 200 MPa. Before compaction, the particle size distribution study by the sedimentation technique on the different spinel-type calcined and atrition-milled powders revealed that the measured average agglomerate size, as it is shown in Fig. 6, ranged from about 2 μm for the 218 and 1218 spinel-type powder compositions, up to an average agglomerate size as high as 5 μm in the case of the 614 spinel-type powder composition. After compaction, the density of the green compacts was very similar being these of 48.5, 47, and 50% of the theoretical density for the 218, 614, and 1218 powder samples, respectively.

Fig. 7 shows the linear shrinkage (a) and linear shrinkage rate (b) under the CRH sintering conditions of 218, 614, and 1218 samples, in air. From the broad sintering range shown in the three samples it can be assumed as representative a solid-state sintering process in all cases. Although the powders had been calcined at the same conditions (750 °C for 2 h), the 218 sample exhibited a lower onset temperature of rapid densification due to its smaller agglomerate size. However, the 1218 sample showed the highest densification rate and reached its end density at a significantly lower temperature than the two other samples. Furthermore, the linear shrinkage rate demonstrates clearly only one sintering event in the case of the 218 and 1218 samples, while the corresponding curve for 614 sample has two sintering events. The linear shrinkage rate of the 614 sample also has a broader feature and the densification rate is lower than for the 218 and 1218 samples, which indicates a much more sluggish densification, i.e., higher sintering temperatures are required for those powder samples with larger average particle (agglomerate) size. On the other hand, it must be emphasized that the highest densified body at the lowest temperature was achieved for the 1218 composition, i.e., for the composition with the higher Co content. Therefore, it seems to be that the Co content promoted an increase in the shrinkage rate and shifting the maximum shrinkage rate to lower temperatures.

Fig. 8 shows the relative density of the sintered samples under isothermal sintering conditions in the temperature range of 900–1200 °C. The holding time at each temperature

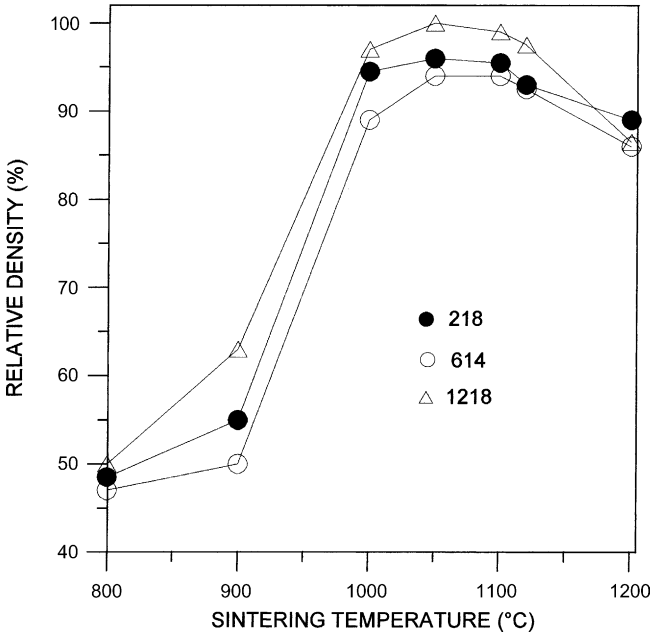

Fig. 8. Temperature dependence of the relative density after 6 h of isothermal sintering for the three $Co_xNiMn_{2-x}O_4$ spinel compositions.

was 6 h. From this figure, two well-established densification regions are to exist. The first one up to 1050 °C, in which the density rapidly increases and the second one, above that temperature, with a decreasing in density as the temperature increases. The 1218 powder composition reaches a relative density as high as 99.9% of theoretical density at only 1050 °C against a 96 and 92% in the case of the 218 and 614 powder compositions, respectively. Above that temperature the relative density decreased for all the compositions but such a decreasing was higher in the case of the 1218 composition, 13%, against 7 and 8.5% in the case of the 218 and 614 compositions respectively, i.e. the higher is the Co content the larger is the density decreasing. Such a de-densification phenomenon above 1050 °C will be discussed later on.

Fig. 9(a)–(e) shows the SEM microstructure studies only for the case of the 1218 spinel composition sintered in the temperature range of 1000–1300 °C for 6 h. As it can be observed, uniform microstructure was developed with a relatively slow grain growth up to a density of about 99.9% at 1050 °C. After heat-treatment above 1130 °C, although the samples still were very dense, a generalized rapid grain growth process took place and, as it can be seen, the grain size increased from about 0.5 μm at 1000 °C, Fig. 9(a), to about 20–25 μm at 1300 °C, Fig. 9(e). Above 1200 °C a small amount of a non-identifiable segregated phase, probably amorphous liquid of a cobalt oxide, could be observed, Fig. 9(d). Average grain size decreases as the Co content increases, i.e., for the same sintering temperature, for example at 1130 °C, the average grain size was about 4, 2.5, and 2 μm for the 218, 614, and 1218 sintered samples, respectively. The exaggerated grain growth present at

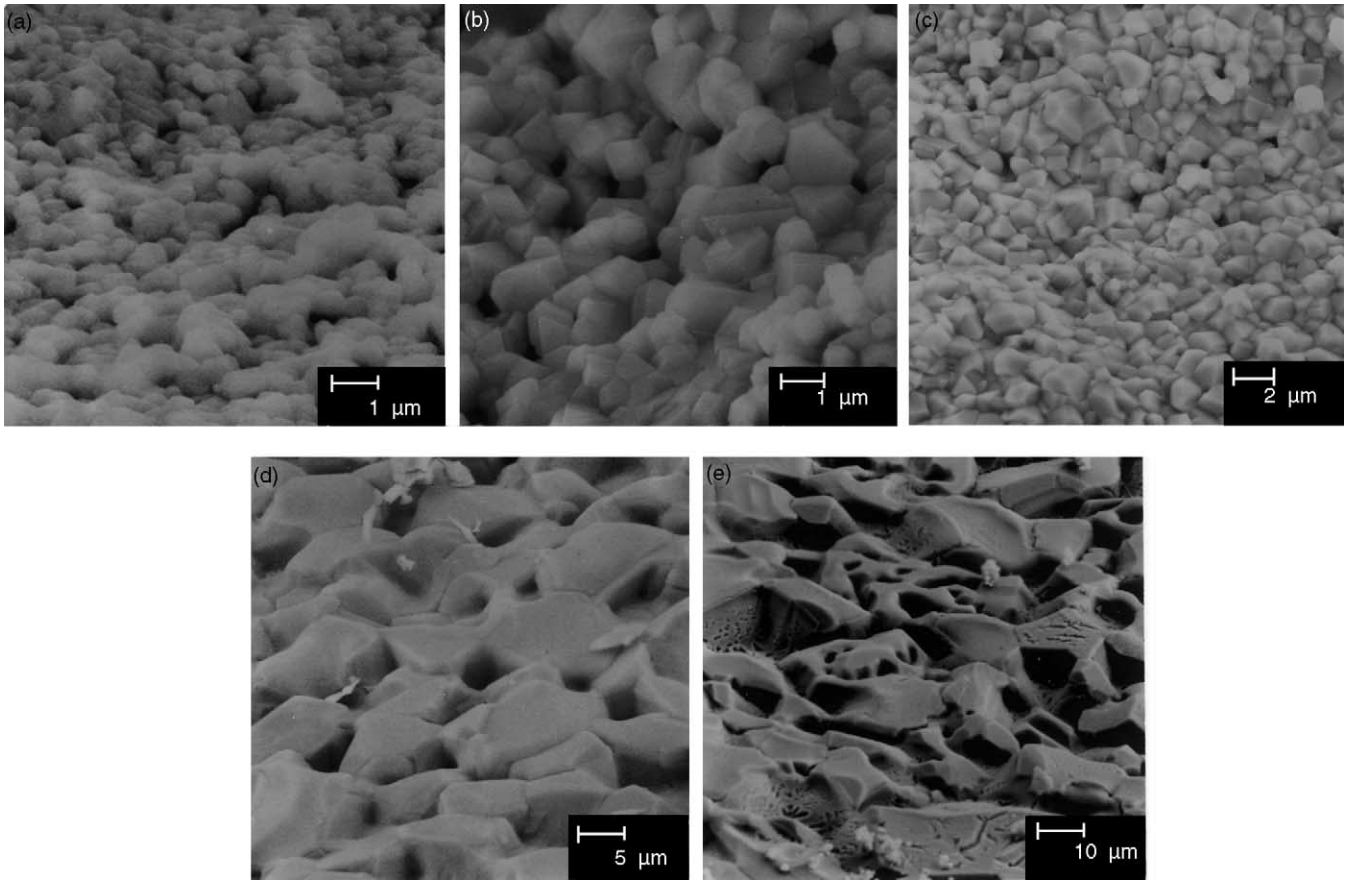

Fig. 9. SEM micrographs of fractured surfaces of 1218 spinel composition sintered for 6 h at 1000 °C (a), 1050 °C (b), 1130 °C (c), 1200 °C (d), and 1300 °C (e) showing abnormal grain growth above 1130 °C.

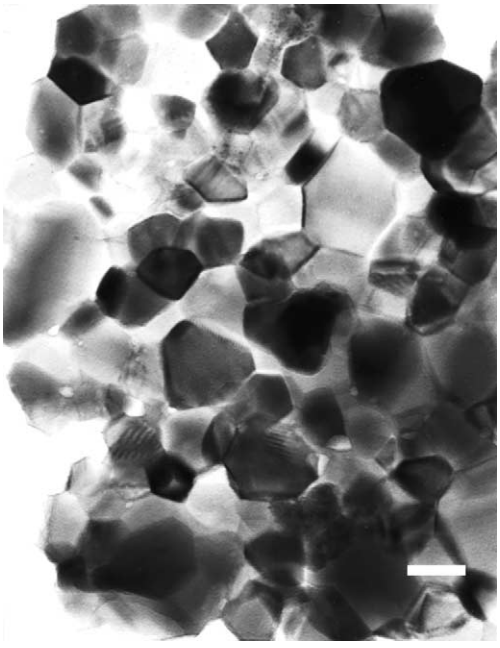

Fig. 10. TEM micrographs of 1218 spinel composition sintered at 1100 °C (bar = 1 μm)

temperatures higher than 1130 °C indicated a very high mobility of grain boundaries.

In order to detect the presence of a possible cobalt oxide boundary film, TEM analysis of the microstructure on the 1218 sample sintered at 1100 °C was performed, as shown in Fig. 10. No liquid phase film could be observed at the present experimental conditions confirming, thus, that the densification process up to or below that temperature is typical of a solid state sintering as previously mentioned.

4. Discussion

A simple and low cost preparation process leading to the low-temperature formation of single-phase in the spinel series $(Co_xNiMn_{2-x})O_4$, by using cheap organic and inorganic reagents as metal nitrates, nitric acid, and ethylene glycol, is proposed. Contrarily to the Pechini's method [8] in which carboxylic acid groups as chelating end groups are to exist in the organic solution, in the used ethylene glycol process, firstly proposed by Anderson et al. [9], it is believed that during the preparation of the polymeric gel at 80 °C and further drying at 130 °C, the ethylene glycol is, at least,

partially oxidized by the nitrate ions leading to the formation of carboxylic acid groups ($HCOO^-$) and/or (–COO–COO–) which can then act as the chelating end groups [10,11]. From the DTA/TG results in Fig. 1, it seems to be that an auto-combustion process accompanied by a strong exothermic reaction in a very narrow temperature range, takes place during the heating of the partially oxidized ethylene glycol–metal nitrate dried polymeric gel, leading to the formation of the spinel-type single-phase at low temperature. It is also stated that such an auto-combustion was catalyzed by the nitrate ions, and took place as consequence of the reaction between the metal nitrate and the formed carboxylic groups through an oxidation-reduction process. According to our XRD studies, see Fig. 2, the heat-treatment of the polymeric gel at 80 and 130 °C did not show the presence of any crystalline peaks corresponding to the formation of formate or oxalate salts, as reported by Chen et al. [10] and Wang et al. [12]. Although it does not preclude the mentioned salt formation but our results indicate that, in the present experimental conditions, we are in the presence of a complex amorphous compound in which the nitrate ions are required to remain in the dried gel to preserve charge balance [13]. As the temperature was increased, it was found that $Co_xNiMn_{2-x}O_4$ spinel-type crystalline phase starts to form at a temperature as low as 263 °C, and any formation of other impurity phases was detected. It is confirmed, thus, from the XRD studies that the spinel $Co_xNiMn_{2-x}O_4$ crystalline phase is found over the whole calcination temperature range and all diffraction peaks are indexed to the diffraction indices of cubic or tetragonal spinel phase. It is also clear from our XRD studies that organic free pure single phase $Co_xNiMn_{2-x}O_4$ powder was obtained at a temperature as low as 400 °C for 2 h. Therefore, this synthesis method results in much lower calcination temperature and shorter calcination time for producing the single phase spinel-type when compared with the conventional solid-state reaction and other solution techniques [4–6].

From our FTIR spectroscopy studies, see Fig. 3, the almost disappearance of the absorption bands attributed to the CH_2 stretching vibration in the 2780–2930 cm^{-1} region, supported the above statement for a partial oxidation of the ethylene glycol. Furthermore, the spectroscopy FTIR analyses also revealed new changes between the spectra of dried gel and the ceramic precursor. For example, the shift of the O–H absorption band at 3399 cm^{-1} to higher wave numbers and the appearance of a new absorption bands at 1630 and 1385 cm^{-1}, associated with the carboxylate groups, leads to assume that some interaction of the metal ions with the O–H groups and maintained chemically bound in the complex polymer amorphous structure has, probably, occurred. Thus, a metal-ion stabilization mechanism similar to that operating in the Pechini's method [8,15], but not necessarily the same, could have taken place. A plausible explanation would be a trapping phenomenon within the ethylene glycol–cation nitrates network structure of the complex polymer, in which some of the cations are coordinated to the formed COO^- groups and, on the other hand, the other cations will be coordinated (stabilized?) to the hydroxyl groups [14–16]. The non-existence of chelating groups in the initial polymerized complex gel would help to such an interpretation.

After calcining at different temperatures it was demonstrated, based on our SEM/TEM results as shown in Figs. 4 and 5, that the morphology, crystal size, and specific surface areas of the calcined powders were dependent of the chemical composition. These results indicate that, although the used EG amount in all the compositions was enough to trap the whole range of metal cations to make a homogeneous precursor, but some differences in the internal structure of the prepared polymeric gels are probably to exist.

Experimental precise lattice parameters a, measured on the here obtained cubic spinel-type single-phase, were found to be dependent on the Co cation concentrations and decreased as the Co concentration was increased. If we take into account that the ionic radii of the Co^{3+} is 0.685 Å, Mn^{3+} is 0.72 Å, and that of the Ni^{2+} ions is 0.83 Å, it seems reasonable to assume a replacement of the larger Mn^{3+} ions by the smaller Co^{3+} ions in both the tetrahedral A and octahedral B sites of the cation sublattices, with the corresponding decreasing in the lattice parameters [6]. Furhtermore, the manganese cations formed in Mn^{4+} oxidation state, favoured by the low calcination temperature, have ionic radius smaller than that of the Mn^{3+}, and this would also lead to a slight decrease in the unit cell volume. To a first approximation we consider that, in the present experimental conditions, the formed Mn^{3+} and Co^{3+} cations are located in both the tetrahedral A and octahedral B sites, and all the Ni^{2+} cations were in the octahedral B sites within the cubic spinel structure. On this assumption a cation distribution as $[Co_{0.2-x+y}{}^{3+}$-$Mn_{0.8-y+x}{}^{3+}]_A$ $[Ni^{2+}Co_{x-y}{}^{3+}Mn_{1-x+y}{}^{3+}]_BO_4$ for the 218 cubic spinel-type compositions could tentatively be advanced. On the other hand, if the semiconducting properties of these NTC materials implies the existence of Mn^{3+} and Mn^{4+} ions in the octahedral B sites, then a new cation configuration as for example, $[Co_{0.2-x+y}{}^{3+}$ $Mn_{0.8-y+x}{}^{2+}]_A$ $[Ni^{2+}Co_{x-y}{}^{3+}Mn_{0.2-2x+2y}{}^{3+}Mn_{0.8-y+x}{}^{4+}]_BO_4$, should be taken into account. The way in which these cations are substituted will give a measure of the stability of the spinel-type phase [17]. The knowledge of the true preferability of the cation occupation on both tetrahedral A and octahedral B sites is a study, by means of neutron diffraction and magnetic measurements, which is now in progress.

The sintering behaviour of $Co_xNiMn_{2-x}O_4$ spinel-type powders, as shown in Figs. 7 and 8, has been studied in the temperature range 900–1200 °C in air. Our results show evidence for a typical solid state sintering, and theoretically dense $Co_{0.2}NiMn_{1.8}O_4$ materials were achieved at temperatures as low as 1050 °C for 6 h. Above that temperature the densification kinetics during sintering were strongly affected

and a dramatic decrease in the density was present in all spinel ceramic compositions. Such a decrease was higher for the composition with the higher Co content. It is believed that this phenomenon was due to an oxygen loss as consequence of the reduction of Co cations at elevated temperatures according to the following equation:

$$Co_3O_4 \rightarrow 3CoO + 1/2O_2(g)\uparrow$$

such as Co cations reduction changed the sintering mechanism. This behaviour had been also observed in other systems [18–20], and was attributed to a gradual removal of oxygen as consequence of a progressive reduction of Co^{3+} to Co^{2+}. For example, in Co_3O_4-doped ceria ceramic composites, Kleinlogel and Gauckler [19] reported that when the precipitated cobalt nitrate decomposed on the doped ceria crystallite surface, a thin film of Co_3O_4 was formed which melted at a temperature as low as 900 °C. In such a way, the sintering of Co_3O_4-doped ceria composites took place via a liquid phase. A similar explanation was furtherly reported by Fagg et al. [20] for the sintering of Co-modified-doped ceria electrtolytes.

In the case of the $Co_xNiMn_{2-x}O_4$ spinel-type samples sintering, an additional oxygen loss due to the reduction of Mn^{4+} to Mn^{3+} should be taken in to account and, therefore, the bloating phenomena present during sintering of these caramic materials can be better described according to this another equation:

$$(Co^{3+}, Mn^{4+}) \rightarrow (Co^{2+}, Mn^{3+}) + O_2(g)\uparrow$$

4.1. Such a bloating phenomenon was depressed as the Co content decreases in the spinel-type compositions

The microstructure of $Co_xNiMn_{2-x}O_4$ samples sintered in the 900–1130 °C temperature range were essentially composed by polygonysed grains, which supported the evidence of a solid-state phase sintering. Given that no evidence is available for a eutectic liquid-phase in the CoO–NiO–MnO ternary system, the fast densification rate in the samples cannot be related to a liquid-phase sintering process. Therefore, it can be stated that the intermediate-stage sintering mechanism of $Co_xNiMn_{2-x}O_4$ samples is changed as the Co content increases. In such a temperature region a regime of slow grain growth took place and the grain size, not show here, was almost proportional to density. Although such a statement is consistent with the suggestions of Gupta [21], but more experimental data are necessary to be sure of such a correlation. A similar result was reported by Hsieh and Fang [22] who suggested that discontinuous grain growth did not occurs up to a relative density of 99% of theoretical, i.e., well within the final-stage of sintering of $BaTiO_3$ samples. In our case, after the end of the intermediate-stage of sintering, i.e., slightly above 1100 °C, both a rapid grain growth and a desintering phenomenon took place which extended up to 1300 °C, see Figs. 8 and 9. Although a rapid grain growth process is consistent with the final-stage of sintering, but the simultaneous presence of a desintering phenomenon cannot be explained on the only basis of a increasing of the grain size. Just above 1100 °C, a gas releasing (O_2) and simultaneously the beginning of exaggerated grain growth took place. There is a short temperature interval (1130–1200 °C) in which the exaggerated grain growth with a porosity development began, with the subsequent decreasing in relative density. It is clear that, from a thermodynamic point of view, the driven force for densification is depressed supporting, thus, the Xue and Brook [23] analysis. Above 1200 °C, and coinciding with the appearance of a cobalt oxide liquid-phase, the exaggerated grain growth process predominated on the oxygen gas release phenomenon and, being the grain boundary mobility extremely high, the generated pores are entrapped at the interior of the grains, see Fig. 9(d) and (e), and given that the porosity is closed the pores become very difficult to be eliminated giving rise, thus, to a desintering or bloating phenomenon.

Summarising, solid-state sintering with no exaggerated grain growth was observed below 1130 °C, and dense bodies (≥99.9% of theoretical density) with submicronic average grain sizes were achieved in the case of the 1218 spinel composition.

5. Conclusions

The ethylene glycol process has been successfully used to the low-temperature (600–700 °C) preparation of nanosized single-phase of the spinel series $(Co_xNiMn_{2-x})O_4$, where $0.2 \leq x \leq 1.2$. It is stated that during the polymerization process of the precursor solution containing ethylene glycol, nitric acid, and metal nitrates at 80 °C, a partial oxidation of the ethylene glycol takes place giving rise to the formation of carboxylic acid groups. The metal cations would be in this manner trapped within the network complex polymeric gel coordinated to the COO^- groups and or stabilized via interaction with the hydroxyl groups remaining in the aqueous solution. No formate or oxalate compounds were detected after polymerization, and the precursor solution, after drying at 130 °C, led to the formation of an amorphous $CoNiMnNO_3$–$(EG)xH_2O$ powder precursor. The spinel-type single-phase was formed at about 260 °C via an auto-combustion of the partially oxidized ethylene glycol–metal nitrate dried gel precursors. The precursor decomposed completely into the spinel-type phase above 300 °C based on the DTA/TG results. XRD studies showed that nanosized $(Co_xNiMn_{2-x})O_4$ crystalline powder with pure spinel-type structure, as the only phase present, was attained with increasing calcination temperature between 600 and 700 °C. The powder morphology studies, as observed by SEM and TEM, showed that particle size and specific surface areas of the spinel-type calcined powders were dependent of the Co content.

The crystalline structure of the synthesized spinel-type phase had a cubic symmetry for the compositions $(Co_{0.2}NiMn_{1.8})O_4$ and $(Co_{0.6}NiMn_{1.4})O_4$ and tetragonal symmetry for the $(Co_{1.2}NiMn_{0.8})O_4$ composition, and a significant decreasing of the cubic cell volume took place as the Co content increased. A tentative cation distribution for the cubic spinel phase is proposed.

Near fully dense spinel-type ceramic bodies (99.9% of theoretical density) with submicronic grain sizes could be achieved at temperatures as low as 1050 °C for 6 h. The fast densification can be attributable to a change in the intermediate-stage sintering mechanism of $Co_xNiMn_{2-x}O_4$ samples as the Co content increases. Above about 1130 °C, a rapid grain growth with entrapment of pores occurred. Oxygen gas release from the reduction of Co^{3+} and Mn^{4+} to Co^{2+} and Mn^{3+}, respectively, and the high mobility of the grain boundaries were, probably, the cause for the high-temperature desintering phenomenon.

Acknowledgment

The present work was supported by the Project 07N/0096/02 of the Autonomous Community of Madrid (CAM).

References

[1] Y. Abe, T. Meguro, S. Oyamatsu, T. Yokoyama, K. Komeya, Formation region of monophase with cubic spinel-type oxides in Mn–Co–Ni ternary system, J. Mater. Sci. 34 (1999) 4639–4644.

[2] T. Tokoyama, Y. Abe, T. Meguro, K. Komeya, K. Kondos, S. Taneko, T. Sasamoto, Preparation and electrical properties of sintered bodies composed of monophase spinel $Mn_{(2-x)}Co_{2x}Ni_{(1-x)}O_4$ $(0 \leq x \leq 1)$ derived from rock-salt-type oxides, Jpn. J. Appl. Phys. 35 (1996) 5775–5780.

[3] T. Tokoyama, K. Kondo, K. Komeya, T. Meguro, Y. Abe, T. Sasamoto, Preparation and electrical properties of monophase cubic spinel, $Mn_{1.5}Co_{0.95}Ni_{0.55}O_4$, derived from rock-salt-type oxide, J. Mater. Sci. 30 (1995) 1845–1848.

[4] J.L. Martin De Vidales, P. Garcia-Chain, R.M. Rojas, E. Vila, O. Garcia-Martinez, Preparation and charaterization of spinel-type Mn–Ni–Co–O negative temperature coefficient ceramic thermistors, J. Mater. Sci. 33 (1998) 1491–1496.

[5] J. Philip, T.R.N. Kutty, Colossal magnetoresistance of oxide spinels $Co_xMn_{3-x}O_4$, Mater. Lett. 39 (1999) 311–317.

[6] C. Boudaya, l. Laroussi, E. Dahari, J.C. Jouber, A. Cheikh-Rouhou, Preparation and characterization of the spinel series $Co_{6+x}Ni_{4-x}Mn_8O_{24}$ $(0 \leq x \leq 4)$, Phase Transitions 68 (1999) 631–642.

[7] K. Nakamoto, Infrared and Raman spectra of inorganic and coordination compounds, fourth ed., Wiley Press, New York, 1986, p. 231.

[8] M. Pechini, Method of preparing lead and alkaline-earth titanates and niobates and coating method using the same to form a capacitor, U.S. Patent 3 330 697 (July 1967).

[9] H.U. Anderson, M.J. Pennell, J.P. Guha, Polymeric synthesis of lead magnesium niobate powders, in: G.L. Messing, K.S. Mazdiyasni, J.V. McCauley, R.A. Haber (Eds.), Advances in Ceramics, vol. 21: Ceramic Powder Science, American Ceramic Society, Westerville, OH, 1987, pp. 91–98.

[10] C.C. Chen, M.M. Nasrallah, H.U. Anderson, Synthesis and charaterization of $(CeO_2)_{0.8}(SmO_{1.5})_{0.2}$ thin films from polymeric precursors, J. Electrochem. Soc. 140 (1993) 3555–3560.

[11] S. Wang, K. Maeda, M. Awano, Direct formation of crystalline gadolinium-doped ceria powder via polymerized precursor solution, J. Am. Ceram. Soc. 85 (2002) 1750–1752.

[12] S. Wang, M. Awano, K. Maeda, Low-temperature synthesis of Gd-doped ceria powder by polymerized precursor solution, J. Ceram. Soc. Jpn. 110 (2002) 703–709.

[13] H.B. Park, H.J. Kweon, Y.S. Hong, S.J. Kim, K. Kim, Preparation of $La_{1-x}Sr_xMnO_3$ powders by combustion of poly(ethylene glycol)–metal nitrate gel precursors, J. Mater. Sci. 32 (1997) 57–65.

[14] M. Kakihana, M. Arima, M. Yashima, M. Yoshimura, H. Mazaki, H. Yasuoka, Chemical design for funtional multicomponent oxides by polymerized complex method, in: Advances Materials'93, I/A: Ceramic Powders, Corrosion and Advanced Processing, vol. 14a, Elsevier Science, New York, 1994, pp. 801–806.

[15] M. Gulgun, M.H. Nguyen, W.M. Kriven, Polymerized organic–inorganic synthesis of mixed oxides, J. Am. Ceram. Soc. 82 (1999) 556–560.

[16] N. Uekawa, T. Sukegawa, K. Kakegawa, Y. Sasaki, Synthesis of lead nickel niobate–barium titanate system by oxidation of polyethylene glycol–cation complex, J. Am. Ceram. Soc. 85 (2002) 329–334.

[17] J. Tofter, A. Feltz, Investigations on electronically conducting oxide systems XXIV (1): preparation and electrical properties of the spinel series $Cu_zNiMn_{2-z}O_4$, Solid State Ionics 59 (1993) 249–256.

[18] E. Vila, R.M. Rojas, J.L. Martin De Vidales, O. Garcia-Martinez, Estructural and thermal properties of the tetragonal cobalt manganese spinels $Mn_xCo_{3-x}O_4$ $(1.4 < x < 2.0)$, Chem. Mater. 8 (1996) 1078–1083.

[19] C. Kleinlogel, L.J. Gauckler, Sintering and properties of nanosized ceria solid solutions, Solid State Ionics 135 (2000) 567–573.

[20] D.P. Fagg, V.V. Kharton, J.R. Frade, P-type electronic transpòrt in $Ce_{0.8}Gd_{0.2}O_{2-\delta}$: the effect of transition metal oxide sintering aids, J. Electroceram. 9 (2002) 199–207.

[21] T.K. Gupta, Possible correlation between density and grain size during the sintering, J. Am. Ceram. Soc. 55 (1972) 276–277.

[22] H.L. Hsieh, T.T. Fang, Effects of green states on sintering behaviour and microstructural evolution of high purity $BaTiO_3$, J. Am. Ceram. Soc. 73 (1989) 1566–1573.

[23] L.A. Xue, R.J. Brook, Promotion of densification by grain gowth, J. Am. Ceram. Soc. 72 (1989) 341–344.